Eur. Phys. J. D **25**, 95–99 (2003)
DOI: 10.1140/epjd/e2003-00094-8

THE EUROPEAN PHYSICAL JOURNAL D

Determination of transition dipole moments from time–resolved photoelectron spectroscopy

T. Lohmüller[1], M. Erdmann[1], O. Rubner[2], and V. Engel[1,a]

[1] Institut für Physikalische Chemie, Universität Würzburg, Am Hubland, 97074 Würzburg, Germany
[2] Institut für Nanotechnologie, Forschungszentrum Karlsruhe GmbH, Postfach 3640, 76021 Karlsruhe, Germany

Received 3rd January 2003 / Received in final form 28 February 2003
Published online 29 April 2003 –

Abstract. We show how to extract the energy- and coordinate dependence of dipole-moments for a neutral-to-ionic molecular transition from time-resolved photoelectron spectra. The procedure needs the potential surfaces of the neutral and the cationic state which are involved in the ionization process as an input. Given these potentials and the laser parameters it is possible to determine the functional form of the transition dipole moment from the measured time- and energy-resolved transient signals.

PACS. 31.70.Hq Time-dependent phenomena: excitation and relaxation processes, and reaction rates – 33.80.Wz Other multiphoton processes

1 Introduction

Time-resolved photoelectron spectroscopy (TRPES) has evolved into a powerful technique to study the dynamics of molecules. Here, an ultrashort laser pulse (pump) prepares a wave packet in the system and a time-delayed second pulse (probe) leads to ionization. The ejected photoelectrons then can be analyzed with respect to their kinetic energy at different values of the pump-probe delay. The first experiments which were performed with femtosecond resolution were carried out by Cyr and Hayden [1] and by now several groups have shown the usefulness of this method [2–13]; for a comprehensive list of references see the recent review article by Neumark [14]. As an exciting trend, it has now become possible to simultaneously measure the energy and angular distribution of the ejected electrons [15–17]. Also, it was shown that, by using a set of time-delayed ionizing pulses, one can observe the interference of outgoing electron waves thereby clearly distinguishing between optical and matter-wave interferences [18].

The first theoretical studies of pump-probe femtosecond photoelectron spectroscopy were carried out by Seel and Domcke regarding the internal conversion dynamics in pyrazine [19,20]. Similar calculations for diatomic molecules were performed in our group which revealed that temporal changes of nuclear probability densities can be mapped directly onto the spectrum [21–23], a fact which later was confirmed experimentally [2]. Various other theoretical studies have been undertaken [24–28], where most recently the topic of time–resolved photoelectron angular distributions has been addressed [29–32].

We have recently investigated the powers of TRPES finding this technique to be a sensitive tool to determine *e.g.* the influence of chirped pulse excitation on the preparation of vibrational wave packets [33], to detect the result of a quantum target-state preparation obtained *via* optimal control theory [34] or to selectively probe photofragments resulting from multiple dissociation processes [35]. Here we address another quantity, namely, the transition dipole moment between a neutral and an ionic state. This observable, in general, depends on the molecular geometry as well as on the photoelectron energy. Dipole moments for neutral-to-neutral transitions can in principle be calculated using quantum chemical program packages (provided the electronic structure problem for the initial and final states is solved) though the effort to get reliable values is often large. For the neutral-to-ionic transition the calculations need the treatment of a scattering process involving the correlated continuum wave function of the free electron [31,32] and are hence much more demanding.

Time-resolved spectroscopy aims at the detection of structural molecular changes or fragmentation processes in real time. The interpretation of data is usually performed within the Condon approximation which assumes a constant transition dipole moment μ connecting the electronic states involved in the probe transition. Not much attention has been paid to a possible breakdown of this approximation. In most cases and for neutral-to-neutral transitions, a resonant probe excitation is possible only within a single small spatial window depending on the intramolecular coordinates. Within the restricted window,

[a] e-mail: voen@phys-chemie.uni-wuerzburg.de

the coordinate dependence of μ can usually be ignored. The situation where two well separated excitation windows exist already illustrates the importance of a possible coordinate dependence of the transition dipole moment: within the Condon approximation, the pump-probe signal will exhibit maxima of approximately equal height at times when the prepared wave packet passes one or the other excitation window. On the other hand, if μ assumes different values in the two windows, the signal will show maxima of different height or even only one maximum. The situation is different in a direct probe-ionization process where, for sufficiently large photon energy, ionization takes place independently of the localization of the moving wave packet. Here, the Condon approximation yields a delay-time independent total ion signal, an effect which was first pointed out by Seel and Domcke [19,36]. Pump-probe ionization experiments on K_2 [37] and NaI [38] showed that the obtained data could not be explained without the assumption of a coordinate-dependent dipole moment. Also, theoretical work has been reported which stresses the importance of the breakdown of the Condon approximation [31,32].

Below we will demonstrate how, using a combination of experimentally and theoretically derived information, the functional dependence of the dipole moment (for a neutral-to-ionic transition) can be obtained. Section 2 contains the theoretical approach. The latter is illustrated in Section 3 using a numerical example.

2 Theory

We regard a diatomic molecule with vibrational coordinate R, two neutral electronic states ($|0\rangle$, $|1\rangle$) and an cationic state $|I\rangle$. A pump-probe ionization scheme is displayed in Figure 1: a first laser-pulse (ω_1) initiates a transition $|1\rangle \leftarrow |0\rangle$, preparing a wave packet $|\psi_1(t)\rangle$. A time-delayed probe pulse then ionizes the molecule resulting in an ensemble of ionic wave packets $|\psi_E(t)\rangle$. They correspond to the ejection of a photoelectron with kinetic energy E and are labelled accordingly. Provided the dipole approximation holds, these wave packets are given within time-dependent perturbation theory and for times after the probe excitation is finished [39], as (atomic units are employed in what follows):

$$|\psi_E(t)\rangle = \mathrm{e}^{-\mathrm{i}(H_I+E)(t-\tau)}\,|\psi_E(\tau)\rangle, \tag{1}$$

where H_I is the nuclear Hamiltonian in the ionic state, τ is the delay-time and we used the definition

$$|\psi_E(\tau)\rangle = \mathrm{i}\int_{-\infty}^{\infty} \mathrm{d}t\; a_2(t)\;\mathrm{e}^{-\mathrm{i}\omega_2 t}\mathrm{e}^{\mathrm{i}(H_I+E)t} \times \mu_{I1}\;\mathrm{e}^{-\mathrm{i}H_1 t}\,|\psi_1(\tau)\rangle. \tag{2}$$

Here μ_{I1} is the projection of the transition dipole moment operator on the polarization vector of the electric field, ω_2 is the probe-laser frequency and $a_2(t)$ describes the time-envelope of the laser pulse. The above expression (2) for the nuclear wave function assumes a separation of the photoelectron from all additional particles so that its total energy is given simply by its kinetic energy E [19,20].

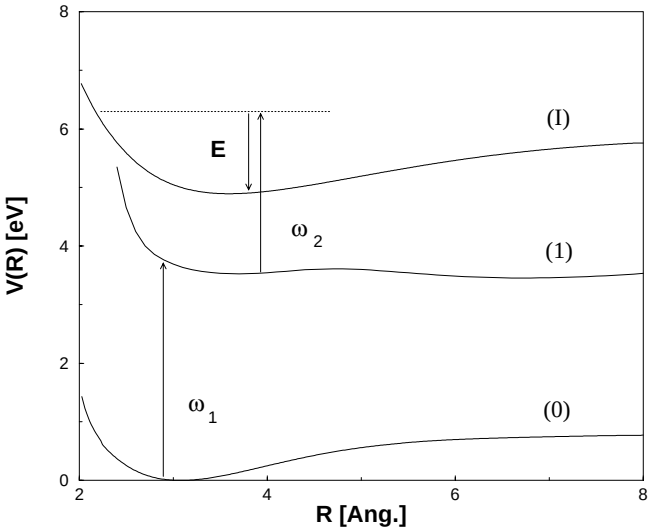

Fig. 1. Pump-probe ionization scheme for a diatomic molecule: an ultrashort laser pulse (pump, ω_1) induces a transition from the electronic ground state $|0\rangle$ to an excited state $|1\rangle$. After a time-delay ionization takes place through the interaction with a second pulse (probe, ω_2). During this process photoelectrons are produced with different kinetic energies E and molecules are prepared in the cationic electronic state $|I\rangle$. The displayed potential curves correspond to electronic states of the Na_2 molecule.

The time-resolved photoelectron spectrum is defined as

$$P(\tau, E) = \langle\psi_E(\tau)|\psi_E(\tau)\rangle. \tag{3}$$

An approximate equation for the ionic wave function can be obtained if commutators between the operators H_I, H_1 and μ_{I1} are ignored [40–43], so that

$$\mathrm{e}^{\mathrm{i}H_I t}\;\mu_{I1}\;\mathrm{e}^{-\mathrm{i}H_1 t} \sim \mu_{I1}\;\mathrm{e}^{\mathrm{i}D_{I1}t}, \tag{4}$$

where $D_{I1}(R) = V_I(R) - V_1(R)$ is the difference potential.

Within the approximation of equation (4) which is valid for short pulses and becomes exact for a constant difference potential, the photoelectron spectrum takes the form

$$P(\tau, E) = \int \mathrm{d}R\;|I(R,E)\;\psi_1(R,\tau)\;\mu_{I1}(R,E)|^2, \tag{5}$$

with the Fourier-integral

$$I(R,E) = \int_{-\infty}^{\infty} \mathrm{d}t\;\mathrm{e}^{\mathrm{i}(D_{I1}(R)-(\omega_2-E))t}\;a_2(t). \tag{6}$$

Using the abbreviations

$$M(R,E) = |\mu_{I1}(R,E)|^2 \tag{7}$$

and

$$g(R,\tau,E) = |I(R,E)\;\psi_1(R,\tau)|^2, \tag{8}$$

the photoelectron spectrum can be written as

$$P(\tau, E) = \int \mathrm{d}R\; g(R, \tau, E)\; M(R, E). \tag{9}$$

Suppose now, that the potential curves of the involved neutral and ionic states (see Fig. 1) are available. If, furthermore, the parameters of the pump- and probe-pulse are known, the function $g(R, \tau, E)$ can be calculated by solving the time–dependent Schrödinger equation. On the other hand, we assume that a measurement that can be routinely performed [2–13] provides the spectrum for a set of energies E_i and delay-times τ_m. In order to determine the modulus squared of the R- and E-dependent transition dipole function from the measured spectrum and the calculated function g, we discretize the integral equation (9) as

$$P(\tau_m, E_i) \sim \Delta R \sum_n g(R_n, \tau_m, E_i)\; M(R_n, E_i). \tag{10}$$

Defining the matrix

$$G(E_i) = \begin{pmatrix} g(R_1, \tau_1, E_i) & \ldots & g(R_1, \tau_N, E_i) \\ \ldots & \ldots & \ldots \\ g(R_N, \tau_1, E_i) & \ldots & g(R_N, \tau_N, E_i) \end{pmatrix}, \tag{11}$$

the unknown vector $M(R_n, E_i)$ can be calculated for a fixed value of the energy E_i:

$$\begin{pmatrix} M(R_1, E_i) \\ \ldots \\ M(R_N, E_i) \end{pmatrix}^t = \frac{1}{\Delta R}\; (G(E_i))^{-1}\; \begin{pmatrix} P(\tau_1, E_i) \\ \ldots \\ P(\tau_N, E_i) \end{pmatrix}. \tag{12}$$

The solution of the matrix equation allows for the determination of the coordinate dependence of the transition dipole moment. In addition, if the procedure is repeated for a different energy, a possible dependence on E can be extracted.

If, on the other hand, the delay time τ_m is fixed and different values of the photoelectron energies are employed, one finds:

$$\begin{pmatrix} M(R_1, E_1) \\ \ldots \\ M(R_N, E_N) \end{pmatrix}^t = \frac{1}{\Delta R} (G(\tau_m))^{-1}\; \begin{pmatrix} P(\tau_m, E_1) \\ \ldots \\ P(\tau_m, E_N) \end{pmatrix}, \tag{13}$$

where the appearing matrix is of the form

$$G(\tau_m) = \begin{pmatrix} g(R_1, \tau_m, E_1) & \ldots & g(R_1, \tau_m, E_N) \\ \ldots & \ldots & \ldots \\ g(R_N, \tau_m, E_N) & \ldots & g(R_N, \tau_m, E_N) \end{pmatrix}. \tag{14}$$

We note that, using the latter equation, it is not possible to separate the coordinate– from the energy–dependence. However, the energy dependence of the transition dipole moment is expected to be weak for a direct ionization process so that one may extract the variation of the dipole moment with the bond length also using equation (13).

The feasibility of the approach as outlined above is best illustrated using a numerical example which we present in the next section.

3 Numerical application

As an example we apply the above described scheme to the Na_2 molecule. The potential curves for the $^1\Sigma_g^+$ electronic ground state [45], the double minimum state $^1\Sigma_u^+$ [46,47] and the ionic ground state $^2\Sigma_g^+$ [48] are shown in Figure 1. The pump-probe ionization spectroscopy involving the double minimum state as an intermediate state has been carried out experimentally [49,50]. Very recently, time-resolved photoelectron spectra have been obtained in the group of Baumert [51]. Also, theoretical investigations were performed [22,31].

We have calculated time-resolved photoelectron spectra using Gaussian pump- and probe-pulses where the field envelope had a full width at half maximum of 50 fs. The pump wavelength was set to 332 nm and the probe wavelength was chosen to be 430 nm. The time-dependent Schrödinger equation was integrated employing standard numerical procedures [44]. We used time-dependent perturbation theory to describe the pump process and the spectra were obtained using equation (9). The initial state was the $^1\Sigma_g^+$-vibrational ground state and the rotational degree-of-freedom was not included.

An essential quantity in obtaining the transition dipole moment is the coordinate- and energy-dependent window function $I(R, E)$, see equation (6). The modulus squared of the latter is displayed in the upper panel of Figure 2. Note that for a different choice of the probe-pulse wavelength, the contours are identical but shifted vertically. The lower panel contains a contour plot of the modulus squared of the vibrational wave packet which is prepared in the pump process. Its time-evolution is shown over half a vibrational period in the double-minimum potential. Since the photoelectron spectrum is obtained as an integral over the wave function times the window function it can be directly inferred from the figure that the spectrum shifts as the wave packet changes its position. This is the basic idea of time–resolved photoelectron spectroscopy [19,20,23].

Regard now equation (12): in order to avoid singularities when inverting the matrix $g(R_n, \tau_m, E_i)$ one has to ensure, that the discrete delay times τ_m are chosen such that the spectrum is non-zero for the predefined energyE_i at all considered delay-times. Obviously, when $g(R_n, \tau_m, E_i)$ is zero for the given energy we cannot extract any information about the dipole moment.

Also, one has to take a sufficiently large number of delay-times τ_m into account, since this number determines the number of points R_n which, in turn, determine the accuracy with which the photoelectron spectrum is calculated (*e.g.* Eq. (10)). This, of course, restricts the values R_n for which we are able to determine $M(R, E)$. For practical purposes it is necessary, in order to construct the complete functional form of the transition dipole moment, to adjust the set of delay–times and energies as the wave packet moves from shorter to longer distances. This adjustment, however, is straightforward to perform since the proper choice of parameters can immediately be taken from Figure 2. As an example we choose a fixed energy of $E = 1.3$ eV, see Figure 2. Here the window

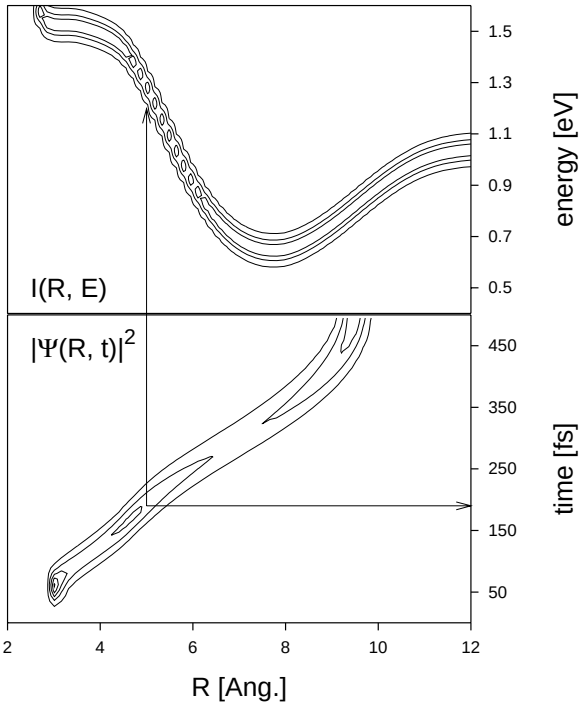

Fig. 2. Upper panel: contour diagram of the energy- and coordinate-dependent window function $I(R, E)$, as defined in equation (6). Lower panel: contour lines of the modulus squared of the vibrational wave packet $\psi(R, t)$ in state $|1\rangle$. In the shown time-interval, the packet moves about half a vibrational period. The arrows indicate that at a delay time of ∼200 fs, where the wave packet is located around an average position of 5 Å the photoelectron spectrum assumes nonzero values at an energy of ∼1.3 eV.

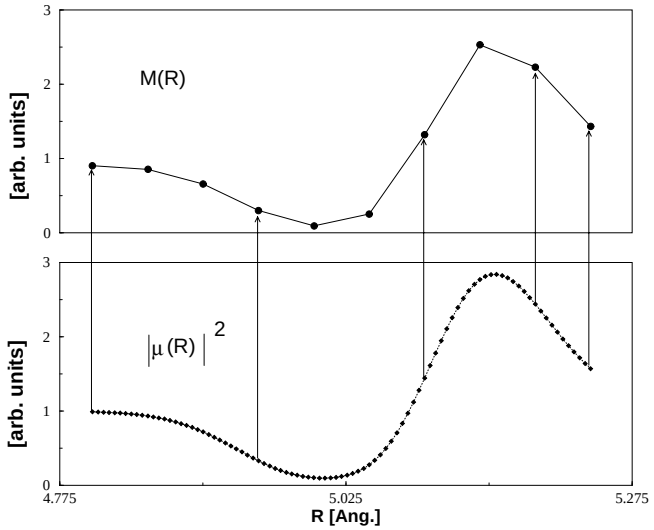

Fig. 3. Upper panel: constructed modulus squared of R-dependent transition dipole moment. Here the photoelectron spectrum at a fixed energy was taken at 10 different times, yielding 10 values of the dipole function. Lower panel: modulus squared of the parameterized transition dipole moment which entered into the numerical calculation of the photoelectron spectrum.

function is nonzero in a range of ∼4.5–5.5 Å. The wave packet is located in this spatial window at delay times between 150 and 250 fs. The matrix inversion as defined in equation (12) will thus yield the coordinate dependence of $|\mu(R, E)|^2$ for the chosen energy at the values of R as detailed above.

We have chosen various forms of a coordinate-dependent transition dipole moment and calculated time-resolved photoelectron spectra. The latter were then used to reconstruct the dipole moment. In the numerical procedure we neglected the energy dependence of the function since its determination is formally equivalent to the calculation of the R-dependence, see equation (12). By adjusting the energy E and the delay-times we were able to construct the entire dipole function in the range of R which is accessible by the wave-packet motion (from about 3 to 9 Å for the laser parameters as used in the simulation).

Let us explore the sensitivity of the method by choosing a numerically demanding example. The lower panel of Figure 3 displays a dipole-moment which, over a small range of 0.4 Å, shows a small deviation from a constant value. Such an behaviour could occur if *e.g.* the neutral electronic state is influenced by a non–adiabatic coupling to a close lying state of the same symmetry (this indeed is the case for our model system, although the coupling region is larger, see Fig. 1). The functional form of the dipole-moment was chosen to be

$$\mu(R, E) = 1 + 8(R - R_0)\, \mathrm{e}^{-\alpha(R-R_0)^2}, \qquad (15)$$

with the particular values of $R_0 = 5.08$ Å and $\alpha = 0.2$ Å^{-2}.

We will not discuss matters of experimental resolution since it is intuitively clear that the presence of large noise will forbid finer structures to be resolved. The upper panel of Figure 3 shows the reconstructed function $M(R, E_f)$. It was obtained by varying the delay-time in an interval from 170 to 215 fs in steps of 5 fs and using the fixed energy $E_f = 1.28$ eV. In this example the construction works excellent.

In summary, we have proposed a numerical method to extract the energy- and coordinate dependence of the transition dipole moments for neutral-to-ionic transitions from available photoelectron spectra. The procedure can be applied if the photoelectron spectra are measured sufficiently accurate and if the potential energy surfaces are known, such that a calculation of these spectra can be carried out. The dipole function is obtained *via* a matrix inversion. The transition moment cannot be obtained in a single step. Due to this limitation the construction has to be repeated for varying bondlengths, thereby choosing proper values of the photoelectron energy and the delay-time.

This work was funded by the Deutsche Forschungsgemeinschaft within the Graduiertenkolleg "Electron density". We gratefully acknowledge support by the Fonds der Chemischen Industrie.

References

1. D.R. Cyr, C.C. Hayden, J. Chem. Phys. **104**, 771 (1996)
2. A. Assion, M. Geisler, J. Helbing, V. Seyfried, T. Baumert, Phys. Rev. A **54**, R4605 (1996)
3. B.J. Greenblatt, M.T. Zanni, D.M. Neumark, Chem. Phys. Lett. **258**, 523 (1996)
4. P. Ludowise, M. Blackwell, Y. Chen, Chem. Phys. Lett. **258**, 530 (1996)
5. C. Jouvet, S. Martrenchard, D. Solgadi, C. Dedonder-Lardeux, M. Mons, G. Grégoire, I. Dimicoli, F. Piuzzi, J.P. Visticot, J.M. Mestdagh, P. D'Oliveira, P. Meynadier, M. Perdrix, J. Phys. Chem. A **101**, 2555 (1997)
6. V. Blanchet, A. Stolow, J. Chem. Phys. **108**, 4371 (1998)
7. J.A. Davies, J.E. LeClaire, R.E. Continetti, C.C. Hayden, J. Chem. Phys. **111**, 1 (1999)
8. P. Farmanara, W. Radloff, V. Stert, H.-H. Ritze, I.V. Hertel, J. Chem. Phys. **111**, 633 (1999)
9. T. Frohnmeyer, M. Hofmann, M. Strehle, T. Baumert, Chem. Phys. Lett. **312**, 447 (1999)
10. M.T. Zanni, A.V. Davis, C. Frischkorn, M. Elhanine, D.M. Neumark, J. Chem. Phys. **112**, 8847 (2000)
11. S. Lochbrunner, T. Schultz, M. Schmitt, J.P. Shaffer, M.Z. Zgierski, A. Stolow, J. Chem. Phys. **114**, 2519 (2001)
12. V. Stert, P. Farmanara, H.-H. Ritze, W. Radloff, K. Gasmi, A. Gonzalez-Urena, Chem. Phys. Lett. **337**, 299 (2001)
13. A.V. Davis, R. Wester, A.E. Bragg, D.M. Neumark, J. Chem. Phys. **117**, 4282 (2002)
14. D.M. Neumark, Ann. Rev. Phys. Chem. **52**, 255 (2001)
15. T. Suzuki, L. Wang, H. Kohguchi, J. Chem. Phys. **111**, 4859 (1999)
16. J.A. Davies, R.E. Continetti, D.W. Chandler, C.C. Hayden, Phys. Rev. Lett. **84**, 5983 (2000)
17. M. Tsubouchi, B.J. Whitaker, L. Wang, H. Kohguchi, T. Suzuki, Phys. Rev. Lett. **86**, 4500 (2001)
18. M. Wollenhaupt, A. Assion, D. Liese, Ch. Sarpe-Tudoran, T. Baumert, S. Zamith, M.A. Bouchene, B. Girard, A. Flettner, U. Weichmann, G. Gerber, Phys. Rev. Lett. **89**, 173001 (2002)
19. M. Seel, W. Domcke, Chem. Phys. **151**, 59 (1991)
20. M. Seel, W. Domcke, J. Chem. Phys. **95**, 7806 (1991)
21. C. Meier, V. Engel, Chem. Phys. Lett. **212**, 691 (1993)
22. C. Meier, V. Engel, J. Chem. Phys. **101**, 2673 (1994)
23. N.E. Henriksen, V. Engel, Int. Rev. Phys. Chem. **20**, 93 (2001)
24. J. Schön, H. Koeppel, J. Phys. Chem. A **103**, 8579 (1999)
25. M. Hartmann, J. Pittner, V. Bonačić-Koutecký, J. Chem. Phys. **114**, 2106 (2001)
26. M. Hartmann, J. Pittner, V. Bonačić-Koutecký, J. Chem. Phys. **114**, 2123 (2001)
27. M. Hartmann, R. Mitric, B. Stanca, V. Bonačić-Koutecký, Eur. Phys. J. D **16**, 151 (2001)
28. M.-C. Heitz, G. Durand, F. Spigelman, C. Meier, J. Chem. Phys. **118**, 1282 (2003)
29. T. Seideman, J. Chem. Phys. **107**, 7859 (1997)
30. T. Seideman, Ann. Rev. Phys. Chem. **53**, 41 (2002)
31. Y. Arasaki, K. Takatsuka, K. Wang, V. McKoy, Chem. Phys. Lett. **302**, 363 (1999)
32. Y. Arasaki, K. Takatsuka, K. Wang, V. McKoy, J. Chem. Phys. **112**, 8871 (2000)
33. Z. Shen, I. Boustani, M. Erdmann, V. Engel, Chem. Phys. Lett. **339**, 362 (2001)
34. Z. Shen, V. Engel, Chem. Phys. Lett. **358**, 344 (2002)
35. M. Erdmann, O. Rubner, Z. Shen, V. Engel, Chem. Phys. Lett. **341**, 338 (2001)
36. V. Engel, Chem. Phys. Lett. **178**, 130 (1991)
37. H. Schwoerer, R. Pausch, M. Heid, V. Engel, W. Kiefer, J. Chem. Phys. **107**, 9749 (1997)
38. G. Grégoire, M. Mons, I. Dimicoli, F. Piuzzi, E. Charron, C. Dedonder-Lardeux, C. Jouvet, S. Martrenchard, D. Solgadi, A. Suzor-Weiner, Eur. Phys. J. D **1**, 187 (1998)
39. V. A. Ermoshin, V. Engel, Eur. Phys. J. D **15**, 413 (2001)
40. M. Braun, C. Meier, V. Engel, J. Chem. Phys. **103**, 7907 (1995)
41. E.M. Hiller, J.A. Cina, J. Chem. Phys. **105**, 3419 (1996)
42. L.W. Ungar, J.A. Cina, Adv. Chem. Phys. **100**, 171 (1997)
43. S. Dilthey, S. Hahn, G. Stock, J. Chem. Phys. **112**, 4910 (2000)
44. M.D. Feit, J.A. Fleck, A. Steiger, J. Comp. Phys. **47**, 412 (1982)
45. A.J. Taylor, K.M. Jones, A.L. Schawlow, J. Opt. Soc. Am. B **73**, 994 (1983)
46. D.L. Cooper, R.F. Barrow, J. Verges, C. Effantin, J. d'Incan, Can. J. Phys. **63**, 1543 (1984)
47. J. Verges, C. Effantin, J. d'Incan, D.L. Cooper, R.F. Barrow, Phys. Rev. Lett. **53**, 46 (1984)
48. C. Bordas, P. Labastie, J. Chevaleyre, M. Broyer, Chem. Phys. **129**, 21 (1989)
49. A. Assion, T. Baumert, V. Seyfried, V. Weiss, E. Wiedenmann, G. Gerber, Z. Phys. D **36**, 265 (1996)
50. A. Assion, T. Baumert, M. Geisler, V. Seyfried, G. Gerber, Eur. Phys. J. D **4**, 145 (1998)
51. T. Baumert, personal communication